

Description of the high spin states in ^{146}Gd using the optimized Woods-Saxon potential

Jerzy Dudek, Zdzislaw Szymański, and Tomasz Werner

Institute for Theoretical Physics, Warsaw University, Hoza 69, PL-00-681 Warsaw, Poland

Amand Faessler and Celso Lima*

Institut für Theoretische Physik, Universität Tübingen, D-7400 Tübingen, West Germany

(Received 6 October 1981)

The Woods-Saxon potential is employed to interpret the properties of single particle and high spin spectra of ^{146}Gd . Spin orbit potential parameters are found which simultaneously reproduce the experimental yrast and yrare states up to $I \sim 18$ and generate the proton single particle energy gap $\delta_p = 2.0$ MeV. The spin-orbit potential parameters obtained are nearly identical for neutrons and protons and are close to the parameter values obtained previously by optimizing the potential to high spin spectra in the vicinity of ^{208}Pb . Properties of the pairing correction method, the Bardeen-Cooper-Schrieffer approximation with blocking, and the particle number projection are discussed and illustrated. It is demonstrated that including the particle number projection term in the total energy formula improves considerably the average slope of the calculated yrast line. The possibility of the collective quadrupole vibrational states becoming yrast states is studied for $I \gtrsim 7\hbar$ using the random phase approximation but only a rather weak effect of collectivity is found in the spin-range studied.

[NUCLEAR STRUCTURE ^{146}Gd ; Woods-Saxon single-particle levels,
high spin excitations. Collectivity in the high spin states, RPA.]

I. INTRODUCTION

The present paper extends a series of studies¹⁻⁴ aiming at the description of single particle nuclear levels in terms of the deformed Woods-Saxon potential. Here we concentrate on the optimization of the potential parameters for ^{146}Gd and its immediate neighbors in analogy to Ref. 4, where ^{208}Pb and the neighboring nuclei have been studied.

The $Z \approx 64$ and $N \approx 82$ region of nuclei is of particular interest from both the experimental and theoretical points of view. Recent experiments (Ref. 5 and references therein) suggest a relatively large single particle energy gap in the proton spectrum corresponding to $Z=64$ (gadolinium). A characteristic lowering of the collective 3^- excitation⁶ ($E_{3^-} = 1579$ keV) lying below the first 2^+ state⁷ ($E_{2^+} = 1971$ keV) reminds one of the properties of the lowest excitations of ^{208}Pb and suggests possible further analogies between the spectra of the two nuclei as, e.g., the domination of the single particle nature in their high spin states. These effects

were in fact discussed extensively in Refs. 5 and 8.

An interesting qualitative difference seems to exist, however, between the two nuclei: While the $Z=82$ and $N=126$ energy gaps are big enough to diminish the nuclear pairing effects to zero, the $Z=64$ gap is significantly smaller and, as a consequence, a relatively strong effect of proton pairing can be expected. In contrast to the proton spectrum, the $N=82$ gap in ^{146}Gd appears too big to produce the neutron pairing correlations. Thus the high spin spectra of ^{146}Gd and some of the $N=82$ isotones contain no pairing contribution from neutrons and relatively "clean" pairing contributions from protons. Previous investigations based on the shell correction method and the Woods-Saxon single particle spectra have shown⁹ that the calculated average slopes of the yrast lines were systematically too low as compared to the experimental ones, at least in the nuclei studied. Nevertheless, the structure of the spectra, such as, e.g., spin-parity interpretation of the yrast states, was given rather well. Since pairing was neglected in these calculations it

was interesting to examine the pairing effect on the yrast spectra in more detail, and ^{146}Gd and some of its isotones can be considered the best candidates for such a study.

The pairing affect was already taken into account in high spin calculations of this type by several authors (see, e.g., Refs. 10 and references therein); we differ from these authors in optimizing the single particle Woods-Saxon potential parameters first. Based on the "optimal" single particle spectra we discuss the treatment of pairing in the next step. Our method of calculation differs also from the one in Ref. 11 where the proton single particle spectra near $Z=64$ have been studied. These differences become more apparent in the discussion below.

II. METHOD OF CALCULATIONS AND RESULTS

The applied method of calculation is essentially the shell plus pairing correction approach of Strutinsky. We use the realization of this method close to that of Bolsterli and co-workers¹²; some modifications required by the particle-hole nature of the studied excitations resemble those of Ref. 13 (see also below).

The total energy of the nucleus is calculated as a sum of the liquid drop model term (with parameters from Ref. 14) and the shell and pairing correction terms

$$E_{\text{tot}}(I, \beta) = E_{\text{LD}}(\beta) + \delta E_{\text{shell}}(\beta) + \delta E_{\text{pair}}(I, \beta) + \delta E_{p-h}(I, \beta). \quad (1)$$

The expression for the pairing correction δE_{pair} is assumed in the form

$$\delta E_{\text{pair}}(I, \beta) = E_{\text{pair}}(I, \beta) - E_{\text{nopair}}(I, \beta) + F_{\text{proj}}(I, \beta), \quad (2)$$

where the energies $E_{\text{pair}}(I, \beta)$ and $E_{\text{nopair}}(I, \beta)$ are calculated similarly as in Ref. 12. The dependence on spin in E_{pair} (E_{nopair}) originates from broken nucleonic pairs and is accounted for within the BCS formalism by blocking, in summations over single particle levels, the states corresponding to broken pairs.

The projection onto a good particle number was performed approximately using a saddle-point method (as, e.g., in Ref. 15; see also the references therein). It results in the presence of the third term in Eq. (2)

$$F_{\text{proj}}(I, \beta) = -\frac{1}{2} H'' / f'' \quad (3)$$

with

$$H'' = -8G \sum_{v \neq v'} u_v v_v^3 u_{v'}^3 v_{v'} \quad (4)$$

and

$$f'' = -4 \sum_v u_v^2 v_v^2. \quad (5)$$

The coefficients $v_v(u_v)$ are the usual single particle state occupation (nonoccupation) probability amplitudes.

The fact that $E_{\text{LD}} + E_{\text{shell}}$ are taken at spin zero in Eq. (1) implies the presence of the term

$$\delta E_{p-h}(I, \beta) = \sum_p e_p - \sum_h e_h, \quad (6)$$

as can easily be shown; here the indices $p(h)$ run over the particle (hole) states and e_v denotes single particle levels. The total energy expression, Eq. (1), depends implicitly on the single particle levels via δE_{shell} , δE_{pair} , and δE_{p-h} , and thus the quality of this expression depends in a crucial way on the single particle spectrum.⁴

Single particle levels are calculated by solving numerically the Schrödinger equation with the deformed Woods-Saxon potential of Refs. 2 and 3

$$V = \frac{V_0}{1 + \exp[\text{dist}_{\Sigma}(\vec{r})/a]} + \lambda \left[\frac{\hbar}{2Mc} \right]^2 \left\{ \nabla \frac{V_0}{1 + \exp[\text{dist}_{\Sigma_{\text{so}}}(\vec{r})/a_{\text{so}}]} \right\} (\vec{\sigma} \times \vec{p}) + \left(\frac{1}{2} + \tau_3 \right) V_{\text{Coul}}(\beta), \quad (7)$$

where $\text{dist}_{\Sigma}(\vec{r})$ [$\text{dist}_{\Sigma_{\text{so}}}(\vec{r})$] denotes the distance of a point \vec{r} from the surface $\Sigma(\Sigma_{\text{so}})$, the surfaces being defined by

$$\sum_{\Sigma_{\text{so}}} : R(\vartheta) = R_{0/R_{\text{so}}} c(\beta_2, \beta_4) [1 + \beta_2 Y_{20}(\cos \vartheta) + \beta_4 Y_{40}(\cos \vartheta)] \quad (8)$$

with $R_0 = r_0 A^{(1/3)}$. We put, after Rost,¹⁶ $a_{so} = a = 0.7$ fm for both protons and neutrons. The expression $V_{Coul}(\beta_2, \beta_4)$ is defined as a classical electrostatic potential of a uniformly charged drop enclosed by Σ . Similarly as in Ref. 4 we adopt proton and neutron central potential radius parameters from Rost [$(r_0)_p = 1.275$ fm and $(r_0)_n = 1.374$ fm, respectively] and

$$V_0 = V \left[1 \pm \chi \frac{N-Z}{N+Z} \right] \quad (9)$$

with $V = -49.6$ MeV and $\chi = 0.86$. These values reproduce the depths of the central part of the potential obtained by Rost for $Z = 82$ and $N = 126$ and the plus and minus signs hold for protons and neutrons, respectively.

The single particle level order is apparently most sensitive to the spin-orbit part of the potential; one of the most important elements of the analysis here is to reproduce the expected value of the $Z = 64$ energy gap. Since the first noncollective excitations found⁵ in ^{146}Gd are $E^* \approx 3.38$ MeV and have presumably two-quasiparticle character, one can deduce the corresponding gap value δ_p using the BCS approximation

$$E^* \approx \left(\frac{1}{4} \delta_p^2 + \Delta^2 \right)^{1/2} + \left(\frac{1}{4} \delta_p^2 + \Delta^2 \right)^{1/2}, \quad (10a)$$

where

$$\delta_p = \sqrt{(E^*)^2 - 4\Delta^2} \quad (10b)$$

with Δ denoting the usual BCS energy gap. For $\Delta \approx 1.2$ MeV expression (10b) gives $\delta_p \approx 2.4$ MeV (Ref. 5). This value agrees also with the δ_p value deduced¹¹ from the ^{145}Eu data.

The calculated proton single particle levels are displayed in Fig. 1 as functions of the spin-orbit potential radius parameter r_{so} for $\lambda_p = 36.0$. Results of Fig. 1 indicate that depending on a particular value of r_{so} one can obtain an energy gap δ_p , for $Z = 64$, ranging between 2.0 and 2.2 MeV. However, the level order and the relative distances among the other single particle levels provide an additional constraint. The actual optimum values of λ and r_{so} have to be selected after taking into account both the energy gap and the order of the single particle levels, and also the results for the high spin spectra described here essentially by particle-hole excitations. (Analogous results for neutrons are shown in Fig. 2 with $\lambda_n = 35.0$.)

The high spin states (yrast and yrare lines) of ^{146}Gd have been calculated minimizing the total en-

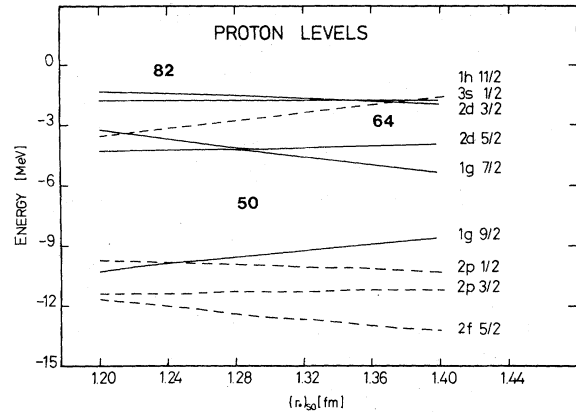


FIG. 1. Proton single particle levels vs spin-orbit potential radius parameter r_{so} for fixed value of $\lambda = 36$. This value of λ was found "optimal," see text. The high spin spectra represented below correspond to $r_{so} = 1.32$ fm.

ergy (1) for each given angular momentum as functions of the deformation. After trying several sets of λ and r_{so} values we arrived at the choice $\lambda_n = 35.0$, $\lambda_p = 36.0$, $(r_{so})_p = 1.32$, and $(r_{so})_n = 1.31$ fm which reproduces the high spin spectrum of ^{146}Gd and the energy gap $\delta_p = 2.0$ MeV simultaneously (for the corresponding single particle level order see Figs. 1 and 2).

In Fig. 3 the resulting yrast and yrare lines are compared with the experimental data. Here the low-lying states with $I < 7\hbar$ are omitted since they are expected to contain strong contributions from the collective 3^- state; the effect of coupling to the collective octupole degrees of freedom is not included in this paper. One can see that the high spin part of the spectrum ($I \geq 7\hbar$) is reproduced rather well. The discrepancies do not exceed 0.5 MeV,

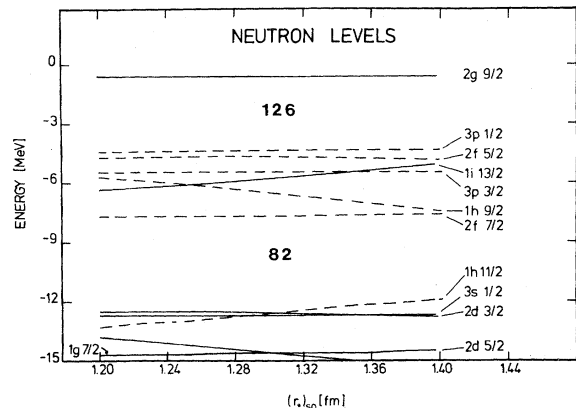


FIG. 2. The same as in Fig. 1 but for the neutrons; $\lambda_n = 35.0$, $r_{so} = 1.31$ fm.

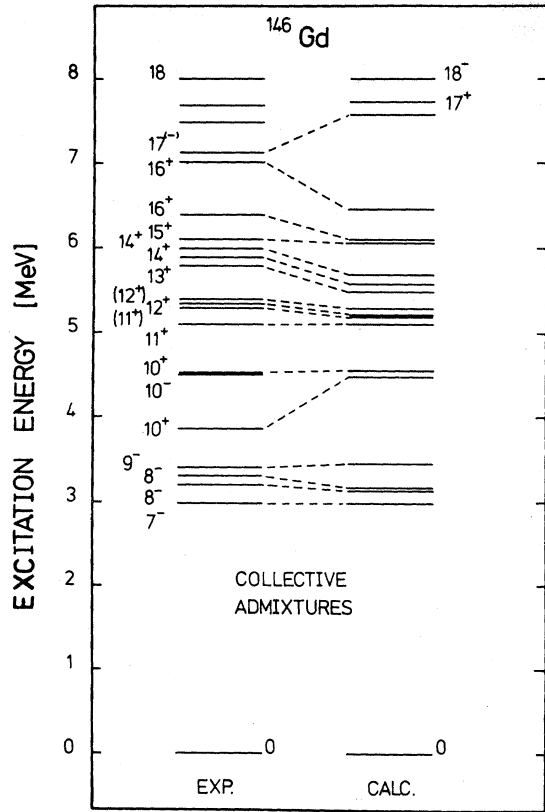


FIG. 3. Calculated yrast and yrare states of ^{146}Gd compared with the experimental data from Refs. 5 and 8; the corresponding shell model configurations are given in Table I.

even around 8 MeV excitation energy.

The deformation of the nucleus as calculated here (see Table I) is close to zero, although a slight increase of the oblate quadrupole deformation with spin is obtained. In addition to the deformations, Table I also lists the shell model configurations of the yrast states. Except for one level (see the table) all the configurations proposed agree with those obtained by making use of the shell model approach (see Ref. 8, and references therein).

The effect of pairing on the yrast line in the present calculations is illustrated in Fig. 4. It can easily be seen that only after accounting for the particle number projection term is the average slope of the yrast line reproduced correctly. It happens frequently that the effect of pairing manifests itself in lowering yrast energies in such a way that the whole spectrum spreads out while the level order remains unchanged. One has to emphasize, however, that in general the calculated configurations of the yrast states may change when including pairing.^{15,10}

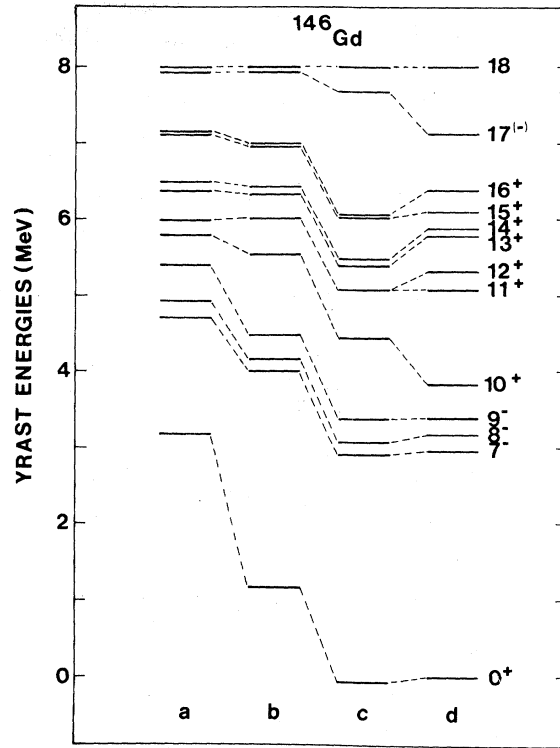


FIG. 4. The role of pairing in the calculations employing liquid drop plus shell correction plus pairing correction method. The results corresponding to neglect of pairing (column a), the results obtained with pairing accounted for but without particle number projection (column b), and the results obtained after including the particle number projection term (column c) are compared to the experimental data (column d). Here only the yrast states are displayed. The spectra were normalized arbitrarily to the experimental $I=18$ energy value. Since according to the calculations there is already no pairing in theoretical 18^- state, this way of normalization shows that the importance of pairing decreases gradually with the number of broken pairs (and, on the average, with increasing spin).

Especially in nuclei with a few proton and neutron particles or holes, outside closed shells pairing can decisively influence the structure of the yrast wave functions. [Note that in ^{146}Gd the lowest excited states (Table I) are composed of particle-hole excitations of protons only.] In this way we can also understand that the shell correction method (with neglected pairing effects) may provide correct configurations of the excited states along yrast lines while the overall slope of the yrast line may remain significantly different from the experimental one.

Let us note also that the pairing force strength

TABLE I. Particle-hole proton configurations of the yrast states in ^{146}Gd calculated with the single particle spectrum corresponding to the set of the Woods-Saxon potential parameters optimized in this paper. Owing to a large $N=82$ single particle energy gap, the ground state neutron configuration was obtained in all the presented yrast states. Numbers in parentheses give the projection of the single particle angular momentum on the symmetry axis. The last column gives the calculated quadrupole deformations. These configurations agree very well with the shell model calculation results presented in Ref. 8, except for the 14^+ state [$(d_{5/2}^{-1}, g_{7/2}^{-1}; h_{11/2}^2)$ in Ref. 8]. Configurations for the 11^+ , 17^- , and 18^- states were not calculated in Ref. 8.

| I^π | Hole states | Particle states | Deformation β_2 |
|---------|--|---|-----------------------|
| 7^- | $2d_{5/2(-3/2)}$ | $1h_{11/2(11/2)}$ | -0.03 |
| 8^- | $2d_{5/2(-5/2)}$ | $1h_{11/2(11/2)}$ | 0 |
| 9^- | $1g_{7/2(-7/2)}$ | $1h_{11/2(11/2)}$ | 0 |
| 10^+ | $2d_{5/2(-1/2)}, 2d_{5/2(+1/2)}$ | $1h_{11/2(9/2)}, 1h_{11/2(11/2)}$ | -0.15 |
| 11^+ | $2d_{5/2(-3/2)}, 2d_{5/2(+1/2)}$ | $1h_{11/2(9/2)}, 1h_{11/2(11/2)}$ | -0.06 |
| 12^+ | $2d_{5/2(-3/2)}, 2d_{5/2(-1/2)}$ | $1h_{11/2(9/2)}, 1h_{11/2(11/2)}$ | -0.06 |
| 13^+ | $2d_{5/2(-5/2)}, 2d_{5/2(-1/2)}$ | $1h_{11/2(9/2)}, 1h_{11/2(11/2)}$ | -0.03 |
| 14^+ | $2d_{5/2(-5/2)}, 2d_{5/2(-3/2)}$ | $1h_{11/2(9/2)}, 1h_{11/2(11/2)}$ | -0.03 |
| 15^+ | $1g_{7/2(-5/2)}, 2d_{5/2(-5/2)}$ | $1h_{11/2(9/2)}, 1h_{11/2(11/2)}$ | -0.03 |
| 16^+ | $1g_{7/2(-7/2)}, 2d_{5/2(-5/2)}$ | $1h_{11/2(9/2)}, 1h_{11/2(11/2)}$ | 0 |
| 17^- | $1g_{7/2(-7/2)}, 2d_{5/2(-1/2)}, 2d_{5/2(+1/2)}$ | $1h_{11/2(7/2)}, 1h_{11/2(9/2)}, 1h_{11/2(11/2)}$ | -0.03 |
| 18^- | $2d_{5/2(-5/2)}, 2d_{5/2(-3/2)}, 2d_{5/2(-1/2)}$ | $1h_{11/2(7/2)}, 1h_{11/2(9/2)}, 1h_{11/2(11/2)}$ | -0.06 |

constants used here were adopted from Ref. 17 and thus originate from the empirical mass differences.

III. COMMENTS ON THE POSSIBLE EFFECT OF NONAXIAL SHAPE VIBRATIONS ON THE HIGH SPIN ENERGIES

On the basis of the previous studies^{15,18,19} one can expect a significant lowering of the energies of at least some of the high spin states, owing to possible collective vibrations of the nucleus. In particular, the quadrupole-type nonaxial shape vibrations were studied in Refs. 15, 18, and 19 and the corresponding energies of the collective states were estimated to be close to the yrast state energies.

A simple possibility to account for these kind of vibrations is to add the corresponding residual interaction term into the total nuclear Hamiltonian considered. For the mentioned quadrupole vibrations this additional term is usually assumed in the form

$$H_{\text{int}} = -\frac{1}{2}\chi \sum_{\mu=\pm 2} \sum_{\rho;v} \hat{Q}_{2\mu}^+(\vec{r}_\rho) \hat{Q}_{2\mu}(\vec{r}_v) \quad (11)$$

and can then be treated approximately using, for in-

stance, the random phase approximation (RPA). The single particle quadrupole operators in the above expression are defined by

$$\hat{Q}_{2\mu}(\vec{r}_\rho) = \left[\frac{4\pi}{5} \right]^{1/2} r_\rho^2 Y_{2\mu}(\vartheta_\rho, \varphi_\rho); \mu = \pm 2. \quad (12)$$

The properties of the RPA procedure applied for calculating the effect of collective excitation on the high spin state energies were discussed in detail in Ref. 15. We calculated the dispersion curves resulting from the RPA formalism for $I \in [7, 18]$ states of ^{146}Gd using the corresponding single particle configuration (Table I) as the vacuum configurations. The characteristic properties of these results are the following:

(a) The neutron contributions to the dispersion functions are relatively low owing to the big $N=82$ single particle energy gap, from which it also follows that the corresponding poles due to particle-hole neutron excitations are far from the vicinity of the $\omega=0$ point.

(b) The spacing between those proton poles which

are close to the $\omega=0$ point is relatively small, and thus, in contrast to the results of Ref. 15 on ^{152}Dy , no significant lowering of the yrast state energies due to quadrupole-quadrupole interaction is obtained in the case of ^{146}Gd for $I \in [7,18]$ states. (See Fig. 5.)

(c) The overall character of the dispersion curves is such that, even if sometimes an RPA solution is noticeably lower than the corresponding "particle-hole" (or quasiparticle excitation) pole energy, the solution is very sensitive to small modifications of the χ value in most of the cases, arguing for a not too significant importance of the studied collective effect.

On the basis of these results we may expect that the quadrupole-quadrupole force Hamiltonian (11) and (12) does not significantly influence the structure of the high spin excitations in ^{146}Gd . Thus the results based on our realization of the single particle model, which are displayed in Figs. 3 and 4, are not significantly altered owing to nonaxial quadrupole shape vibrations and confirm similar negative conclusions of Ref. 19.

IV. SUMMARY AND CONCLUSIONS

In the present paper we optimized the Woods-Saxon single particle potential parameters to describe high spin excitations of spherical or oblate deformed nuclei in the immediate neighborhood of ^{146}Gd . The optimal parameter values obtained for the spin-orbit part of the potential are nearly the same for the neutrons and protons and are very close to the corresponding values of Ref. 4 where ^{208}Pb and the neighboring nuclei have been studied.

The pairing correlations are significant for protons in ^{146}Gd . We treat them by using the BCS method with blocking and an approximate particle number projection. The calculation of the energy is based on the liquid drop plus shell correction plus pairing correction formula (generalized Strutinsky method); it provides a reasonably good description of known yrast and yrare noncollective states up to spin $I \sim 18\hbar$. The energies of about 18 excited levels are in most cases reproduced within 0.2 to 0.3 MeV accuracy. We also find the relatively weak collective effects in high spin states of this nucleus on the basis of the random phase approximation.

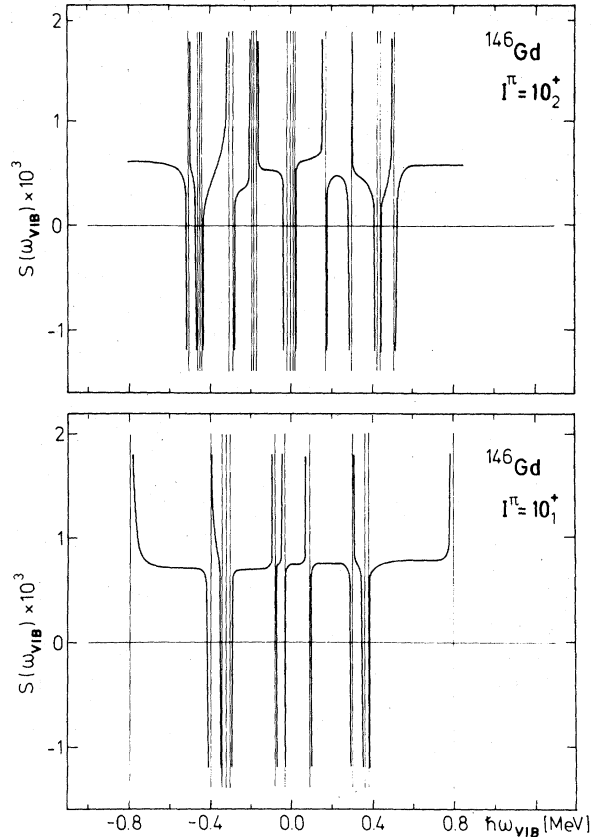


FIG. 5. The dispersion curves for the yrast (bottom) and yrare (top) $I^\pi=10^+$ states. Note small distances between the poles for ω not too far from 0, indicating that only small corrections to the yrast state energies may be expected from the RPA calculations in the nucleus considered. The main properties of the RPA curves for the other $I \in [7,18]$ states in ^{146}Gd are similar and thus one can expect no significant alteration of the single particle character of the high spin excitations in this nucleus, even for a broad range of χ values.

ACKNOWLEDGMENTS

One of the authors (J.D.) wishes to thank the Institute of Theoretical Physics of the University of Tübingen for the hospitality during his stay there. C.L. wishes also to acknowledge the financial support from DAAD and CNPq. This work was supported in part by the Bundesministerium für Forschung und Technologie.

- *On leave of absence from the Universidade Federal do Rio de Janeiro, Brazil.
- ¹J. Dudek and T. Werner, *J. Phys. G* **4**, 1543 (1978).
 - ²J. Dudek, A. Majhofer, J. Skalski, T. Werner, S. Cwiok, and W. Nazarewicz, *J. Phys. G* **5**, 1359 (1979).
 - ³J. Dudek, W. Nazarewicz, and T. Werner, *Nucl. Phys. A* **341**, 253 (1980).
 - ⁴J. Dudek, Z. Szymański, and T. Werner, *Phys. Rev. C* **23**, 920 (1981).
 - ⁵P. Kleinheinz, R. Broda, P. J. Daly, S. Lunardi, M. Ogawa, and J. Blomqvist, *Z. Phys. A* **290**, 279 (1979).
 - ⁶P. Kleinheinz, S. Lunardi, M. Ogawa, and M. R. Maier, *Z. Phys. A* **284**, 351 (1978).
 - ⁷M. Ogawa, R. Broda, K. Zell, P. J. Daly, and P. Kleinheinz, *Phys. Rev. Lett.* **41**, 289 (1978).
 - ⁸P. Kleinheinz, Invited paper, Symposium on High Spin Phenomena in Nuclei, Argonne, 1979, Argonne National Laboratory Report ANL/PHY-79-4, 1979.
 - ⁹M. Cerkaski, J. Dudek, P. Rozmej, Z. Szymański, and S. G. Nilsson, *Nucl. Phys. A* **315**, 296 (1978).
 - ¹⁰T. Døssing, K. Neergard, and M. Sagawa, *Phys. Scr.* **24**, 258 (1981).
 - ¹¹R. R. Chasman, *Phys. Rev. C* **21**, 456 (1980).
 - ¹²R. Bolsterli, E. O. Fiset, J. R. Nix, and J. Norton, *Phys. Rev. C* **5**, 1050 (1972).
 - ¹³G. Andersson, S. E. Larsson, G. Leander, P. Møller, S. G. Nilsson, I. Ragnarsson, S. Aberg, R. Bengtsson, J. Dudek, B. Nerlo-Pomorska, K. Pomorski, and Z. Szymański, *Nucl. Phys. A* **268**, 205 (1976).
 - ¹⁴W. D. Myers and W. Swiatecki, *Nucl. Phys.* **81**, 1 (1966).
 - ¹⁵C. G. Andersson and J. Krumlinde, *Nucl. Phys. A* **291**, 21 (1977).
 - ¹⁶E. Rost, *Phys. Lett.* **26B**, 184 (1968); see also J. Blomqvist and S. Wahlborn, *Ark. Fys.* **16**, 545 (1960); A. Faessler and R. Sheline, *Phys. Rev.* **148**, 1003 (1966).
 - ¹⁷J. Dudek, A. Majhofer, and J. Skalski, *J. Phys. G* **6**, 447 (1980).
 - ¹⁸J. Dudek, Proceedings of the International School of Physics, "Enrico Fermi," Varenna, 1977, edited by Aa. Bohr and R. Broglia (North-Holland, Amsterdam, 1977), p. 469.
 - ¹⁹C. G. Andersson, R. Bengtsson, T. Bengtsson, J. Krumlinde, G. Leander, K. Neergard, P. O. Landers, J. A. Pinston, I. Ragnarsson, Z. Szymański, and S. Aberg, *Phys. Scr.* **24**, 266 (1981).